Bioorg. Med. Chem. 38 (2021) 116138

Contents lists available at ScienceDirect

Bioorganic & Medicinal Chemistry

journal homepage: www.elsevier.com/locate/bmc

Design, synthesis and biological evaluation of novel pleuromutilin derivatives as potent anti-MRSA agents targeting the 50S ribosome

Si-Yu Huang [a], Xiao Wang [a,c], Ding-Yi Shen [a], Fang Chen [a], Guang-Yu Zhang [a], Zhe Zhang [a], Kang Li [a], Zhen Jin [a,b], Dan Du [c,d], You-Zhi Tang [a,b,*]

[a] Guangdong Provincial Key Laboratory of Veterinary Pharmaceutics Development and Safety Evaluation, College of Veterinary Medicine, South China Agricultural University, Guangzhou 510642, China
[b] Guangdong Laboratory for Lingnan Modern Agriculture, Guangzhou 510642, China
[c] Cancer Research Center, School of Medicine, Xiamen University, Xiamen, Fujian, China
[d] Fujian Provincial Key Laboratory of Reproductive Health Research, School of Medicine, Xiamen University, Xiamen, Fujian, China

ARTICLE INFO

Keywords:
Antibacterial activity
MRSA
Pleuromutilin
50S ribosome
SPR
Molecular docking

ABSTRACT

A series of novel pleuromutilin derivatives were designed and synthesized with 1,2,4-triazole as the linker connected to benzoyl chloride analogues under mild conditions. The *in vitro* antibacterial activities of the synthesized derivatives against four strains of *Staphylococcus aureus* (MRSA ATCC 43300, ATCC 29213, AD3 and 144) were tested by the broth dilution method. Most of the synthesized derivatives displayed potent activities, and 22-(3-amino-2-(4-methyl-benzoyl)-1,2,4-triazole-5-yl)-thioacetyl)-22-deoxypleuromutilin (compound **12**) was found to be the most active antibacterial derivative against MRSA (MIC = 0.125 μg/mL). Furthermore, the time-kill curves showed compound **12** had a certain inhibitory effect against MRSA *in vitro*. The *in vivo* antibacterial activity of compound **12** was further evaluated using MRSA infected murine thigh model. Compound **12** exhibited superior antibacterial efficacy than tiamulin. It was also found that compound **12** had no significant inhibitory effect on the proliferation of RAW264.7 cells. Compound **12** was further evaluated in CYP450 inhibition assay and showed moderate inhibitory effect on CYP3A4 (IC_{50} = 3.95 μM). Moreover, seven candidate compounds showed different affinities with the 50S ribosome by SPR measurement. Subsequently, binding of compound **12** and **20** to the 50S ribosome was further investigated by molecular modeling. Three strong hydrogen bonds were formed through the interaction of compound **12** and **20** with 50S ribosome. The binding free energy of compound **12** and **20** with the ribosome was calculated to be −10.7 kcal/mol and −11.66 kcal/mol, respectively.

1. Introduction

The first case of multidrug-resistant *S. aureus* (MRSA) was reported by Jevons in 1961. Since the 1990s, MRSA has spread rapidly in the community.[1] It can cause a variety of infections, such as skin and soft tissue infection, blood stream infection, pneumonia, endocarditis and osteomyelitis.[2] MRSA infections have been reported all over the world, and the prevalence in communities and hospitals continues to rise.[3] The mortality rate for patients with MRSA bacteremia is 20–50%.[4] According to the Centers for Disease Control and Prevention (CDC), it was estimated that nearly 120 000 cases of bloodstream infections were caused by non-invasive MRSA, causing almost 20,000 deaths in the year 2017. MRSA is intrinsically resistant to methicillin and other β - lactam antibiotics. Vancomycin and daptomycin are the first-line antibiotics for the current clinical treatment of MRSA infection.[5] Therefore, it is necessary to develop new antibacterial drugs against this terrible pathogen.

Pleuromutilin (**1**, Fig. 1) is a tricyclic diterpene natural product, which was first isolated from cultures of two basidiomycetes *Pleurotus mutiliz* and *Pleurotus Passeckerianus* by Kavanagh et al. in 1951. Pleuromutilin derivatives show active antibacterial activity against gram-negative bacteria and mycoplasma.[6,7] Pleuromutilin derivatives selectively inhibit bacterial protein synthesis through interacting with the V domain of the peptidyl transferase center (PTC) of the 50S ribosome

* Corresponding author at: College of Veterinary Medicine, South China Agricultural University, No. 483 Wushan Road, Tianhe District, Guangzhou 510642, China.
E-mail address: youzhitang@scau.edu.cn (Y.-Z. Tang).

https://doi.org/10.1016/j.bmc.2021.116138
Received 4 January 2021; Received in revised form 13 March 2021; Accepted 23 March 2021
Available online 2 April 2021
0968-0896/© 2021 Elsevier Ltd. All rights reserved.

subunit.[8] Based on the unique antibacterial mechanism, pleuromutilin and its derivatives possess rarely cross-resistance with other antibiotics used clinically.[9] Thus, pleuromutilin has received considerable attention of researchers as novel and effective antibacterial agents. The structural modifications on the C14 side chain of pleuromutilin has led to the discovery of tiamulin (**2**, Fig. 1) and valnemulin (**3**, Fig. 1), which have been approved as veterinary drugs for poultry and pigs in 1979 and 1999, respectively.[10] Retapamulin (**4**, Fig. 1) was approved as the first pleuromutilin antibiotic for human use to treat skin infections in 2007.[11] Additionally, lefamulin (**5**, Fig. 1) was approved for the treatment of community-acquired bacterial pneumonia (CABP) as the first systemic pleuromutilin antibiotic in 2019.[12]

Previous work in our group has led to several novel pleuromutilin derivatives containing the 2-aminophenylthiol, piperazine ring and 1,2,3-triazole in the C14 side chain. Some of these pleuromutilin analogues displayed potent *in vitro* and *in vivo* antibacterial activity against MRSA (ATCC 43300) and *S. aureus* (ATCC 29213).[13–15] Many 1,2,4-triazoles were included in a wide range of drug applicants with antimicrobial, antioxidant, anti-inflammatory, analgesic and anticancer activities.[16]

This background prompted us to develop novel pleuromutilin derivatives containing 1,2,4-triazole. In this research, we designed and synthesized 20 pleuromutilin derivatives with 1,2,4-triazole as the linker connected to benzoyl chloride analogues, and evaluated their antibacterial activity against 4 strains including MRSA. Among the synthesized derivatives, compound **12** displayed superior antibacterial activity *in vitro* and good efficacy *in vivo* against MRSA. The interaction between compound **12** and 50S ribosome was studied by surface plasmon resonance (SPR) experiments and molecular docking.

2. Results and discussion

2.1. Chemistry

The general synthetic routes for all pleuromutilin derivatives are illustrated in Scheme 1. Compound **6** was firstly synthesized by the reaction between 3-amino-5-mercapto-1,2,4-triazole and compound **8**, which was prepared from pleuromutilin according to previous literature.[17] Compounds **9**–**28** were prepared by condensation reaction of compound **6** with a variety of benzoyl chloride derivatives.

All those pleuromutilin derivatives were purified by silica column chromatography to obtain pure compounds. The structures of those synthesized analogues were characterized by ^{1}H NMR, ^{13}C NMR and high-resolution mass spectral (HR-MS).

The absence of the triazolic NH proton and the presence of two active hydrogen atoms at 6.71 ppm for compound **9**, assigned to the –NH_2 proton in the ^{1}H NMR spectra. The result demonstrated that the nucleophilic acyl substitution occurred on the N2 atom of the 1,2,4-triazole ring instead of the exocyclic amino group (–NH_2). The nucleophilic acyl substitution on the N2 atom of the 1,2,4-triazole ring is more prone to occur under alkaline conditions at room temperature. [18]Chemical shifts of the triazole carbon atoms 3 and 5 of compound 6 were 157.40 and 155.55 ppm. The observed chemical shifts of the triazole carbon atoms 3 and 5 of compound **9**–**28** were around 161 and 158 ppm, and they would not change significantly as compared with those of compound 6. Therefore, the nucleophilic acyl substitution occurred on the N2 atom of the 1,2,4-triazole ring.

2.2. In vitro antibacterial activity

The MIC values of all synthesized pleuromutilin derivatives were tested against MRSA (ATCC 43300), *S. aureus* (ATCC 29213), *S. aureus* (AD3) and *S. aureus* (144) by the broth dilution methods. Tiamulin was used as positive control. The results of these studies were summarized in Table 1.

The MICs of the 21 new pleuromutilin compounds *in vitro* against MRSA (ATCC 43300), *S. aureus* (ATCC 29213), *S. aureus* (AD3) and *S. aureus* (144) ranged from 0.125 to 2 μg/mL, 0.125 to 4 μg/mL, 0.125 to 4 μg/mL and 0.125 to 4 μg/mL, respectively. Among the examined synthesized derivatives, compounds **9, 11, 12, 14, 16, 17** and **20** showed superior antibacterial activity against MRSA compared with tiamulin. Especially, compound **12** was the most active compound in this series. The MIC value of compound **12** was 4 times higher than tiamulin against MRSA. These data indicated that the introduction of 1,2,4-triazole can improve the antibacterial activity of the derivatives.

Compounds **10**–**12** and **16**–**18** were synthesized by introducing electron donating group into benzene ring of compound **9**. Most of these derivatives displayed improved antibacterial activity against MRSA compared with tiamulin. Compounds **13**–**15** and **19**–**28** introduced electron withdrawing groups into the benzene ring of compound **9**. Compared with compound **9**, most of these derivatives showed less antibacterial activity against MRSA. The results showed that the antibacterial activities of the derivatives containing the electron donating group were slightly higher than that of the derivatives containing the electron withdrawing group, which was consistent with previous research.[13]

Due to compounds **12, 14, 16** and **20** have superior MIC values than other pleuromutilin derivatives. The *in vitro* antibacterial activities of these four compounds against MRSA were studied by time-kill kinetics assay. The results of the time-kill curves experiments were presented in

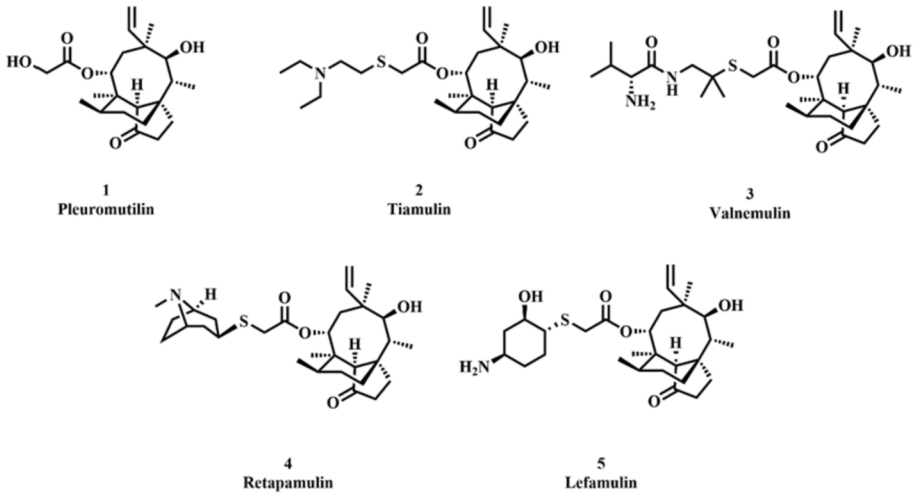

Fig. 1. Structure of pleuromutilin (**1**), tiamulin (**2**), valnemulin (**3**), retapamulin (**4**) and lefamulin (**5**).

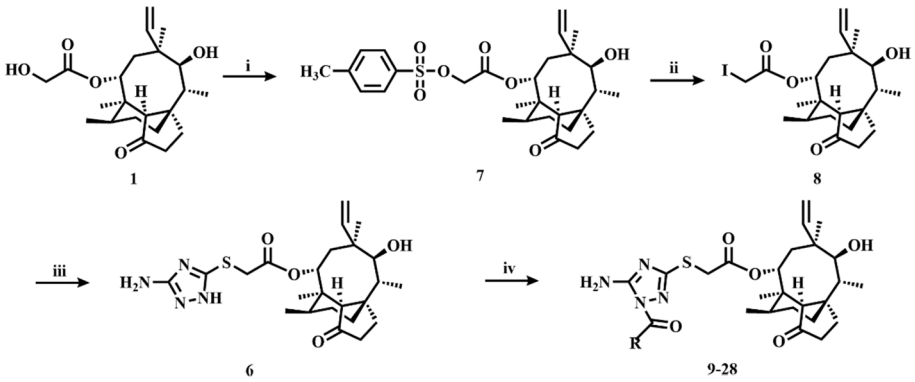

Scheme 1. Reagent and conditions: (i) acetonitrile, *p*-toluenesulfonyl chloride, NaOH, rt, 3 h; (ii) acetonitrile, NaI, 70 ℃, 1 h; (iii) acetonitrile, 3-amino-5-mercapto-1,2,4-triazole, K_2CO_3, 70 ℃, 3 h; (iv) dichloromethane, benzoyl chloride, K_2CO_3, rt, 6 h.

Fig. 2. Compounds **12, 14, 16** and **20** at 4 × MIC induced marked MRSA killing (-1.95 $\log_{10}$ CFU/mL, −1.26 $\log_{10}$ CFU/mL, −2.42 $\log_{10}$ CFU/mL and −1.23 $\log_{10}$ CFU/mL reduction) after 3 h incubation. However, all concentrations did not reach the complete elimination of MRSA at 24 h. The bactericidal effects of these four derivatives on MRSA did not have a positive correlation with the increase in concentration, indicating that the compounds **12, 14, 16** and **20** were not concentration-dependent but time-dependent. For time-dependent antibacterial agents, the dosage can be optimized according to the interval time of each dose to maintain the drug concentration above the MIC of target bacteria.[19]

2.3. *In vivo antibacterial activity*

In order to clarify the *in vivo* antibacterial activity of synthesized compounds against MRSA, the mice thigh infection model was established to evaluate the therapeutic effect. Since compound **12** displayed excellent antibacterial activity *in vitro*, its *in vivo* antibacterial activity was further evaluated using the infection model. Tiamulin was used as positive control and normal saline as negative control. The results of these experiments were shown in Fig. 3. In the infection model, statistical differences were observed on antimicrobial activities against MRSA. Tiamulin (20 mg/kg) could reduce the MRSA load (0.91 ± 0.19 $\log_{10}$ CFU/g) in thighs compared with the no drug control group ($P < 0.0006$, $n = 6$/group). However, compound **12** at the same dose displayed a significant treatment effect (1.89 ± 0.13 $\log_{10}$ CFU/g) against MRSA in thighs compared to no drug control group ($P < 0.0001$, $n = 6$/group). When comparing the bacterial growth of MRSA in control group between tiamulin and compound **12**, the results indicated that compound **12** displayed more effective than tiamulin *in vivo* antibacterial activity against MRSA.

2.4. *Cytotoxicity assay*

By employing the MTT method, the cytotoxic potential of compound **12** and tiamulin were evaluated on RAW 264.7 cells. The cell viability percentages treated with different concentrations of the tested compounds were shown in Fig. 4. The results showed that compound **12** displayed only a slight influence on the viability of RAW 264.7 cells at the concentration was less than 40 μg/mL.

2.5. *Effect on human liver microsomal CYP450 enzyme activity*

Cytochrome P450 (CYP450) is a significant drug-metabolizing enzyme mainly distributed in liver microsomes. It catalyzes many reactions likes xenobiotic metabolism and biosynthesis of cholesterol, steroids, and other lipid components. Once the function of CYP450 enzyme is affected, which might trigger a series of adverse reactions.[20] During the CYP450 enzyme inhibition assessment, compounds with $IC_{50} > 10$ μM are generally considered to be weak CYP inhibitors; compounds with 3 μM $< IC_{50} <$ 10 μM are moderate CYP inhibitors, while compounds with $IC_{50} < 3$ μM are strong CYP inhibitors.[21] Azamulin (Fig. 5a) and tiamulin were reported to possess strong CYP3A4 inhibition effect (IC_{50} values for CYP3A4 were 0.24 μM and 1.60 μM, respectively).[21,22] Therefore, the inhibitory effect of **12** on CYP3A4 was evaluated by determining IC_{50} value in human liver microsomes through the use of testosterone as the probe substrate.

As shown in Fig. 5, compound **12** displayed a moderate inhibitory effect on CYP3A4 ($IC_{50} = 3.95$ μM). The result indicated that compound **12** might have less inhibitory effect on the CYP3A4 than that of azamulin and tiamulin. However, due to the complexity of living organisms, it is necessary to further evaluate the inhibitory effect of CYP450 enzyme system *in vivo* to minimize the adverse reactions caused by CYP450 enzyme system.

2.6. *SPR affinity analysis*

To understand the specific interactions between candidate compounds and the 50S ribosome, we performed an affinity measurement using SPR technology. Due to compounds **9**, **11**, **12**, **14**, **16**, **17** and **20** have superior MIC values than tiamulin, these compounds were further studied by SPR. The binding of each compound to the 50S ribosome during each cycle was represented by the response unit (RU) of surface resonance. The association rate constants (K_a) indicated the speed of the binding reaction, the larger the K_a, the faster the binding. A higher dissociation rate constant (K_d) indicated a high dissociate rate and would presumably be difficult to utilize *in vivo*. K_D showed the degree of dissociation of compounds and the 50S ribosome in the equilibrium state. A higher K_D indicated binding affinity was weak between compounds and the 50S ribosome.

The results revealed that the selected compounds bound reversibly to the 50S ribosome with clear association and dissociation phases. Among all these compounds, **11**, **16** and **20** showed strong affinity (10^{-8} M $< K_D < 10^{-5}$ M) for the 50S ribosome. Compounds **9**, **12** and **14** showed middle affinity (10^{-5} M $< K_D < 10^{-3}$ M) and compound **17** showed weak binding capacity with a high K_d.[23] Several compounds showed middle or only weak binding affinity in the SPR assay. The results were not absolutely consistent with MIC values. This might be due to the high affinity between the compound and the binding site, which affects the diffusion and accumulation of compounds, resulting in the decrease of antibacterial activity. The K_a, K_d and K_D of compounds and controls are shown in Table 2. Their binding curves during the test were shown in Fig. 6, as well as the concentration gradient curves were shown in Figure SI 22-29.

Table 1
MIC (μg/mL) values of compounds **6**, **9**–**28** and tiamulin against MRSA (ATCC 43300), *S. aureus* (ATCC 29213), *S. aureus* (144) and *S. aureus* (AD3).

Compound No	R	MIC(μg/mL) MRSA ATCC 43300	*S. aureus* ATCC 29213	*S. aureus* 144	*S. aureus* AD3
6	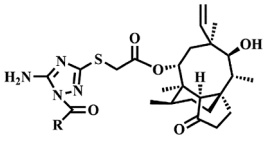	1	1	2	1
9		0.25	1	2	1
10		0.5	1	1	1
11		0.25	0.5	0.5	0.5
12		0.125	0.125	0.125	0.125
13		1	2	4	2
14		0.25	0.5	1	0.5
15	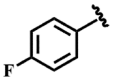	0.5	1	1	1
16	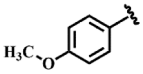	0.25	0.25	0.5	0.25
17	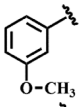	0.25	0.5	0.5	0.5
18	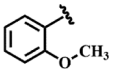	1	1	1	1
19		0.5	0.5	1	0.5
20		0.25	0.25	0.5	0.25
21	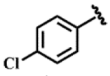	0.5	1	1	1
22	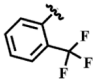	2	4	4	4
23	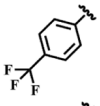	1	1	1	1
24	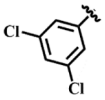	1	1	1	0.5
25	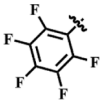	1	2	2	1
26	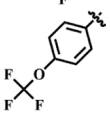	1	2	2	1

(*continued on next page*)

Table 1 (*continued*)

Compound No	R	MIC(μg/mL) MRSA ATCC 43300	*S. aureus* ATCC 29213	*S. aureus* 144	*S. aureus* AD3
27	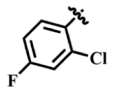	1	1	1	0.5
28	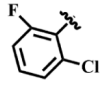	1	2	2	2
Tiamulin		0.5	1	1	1

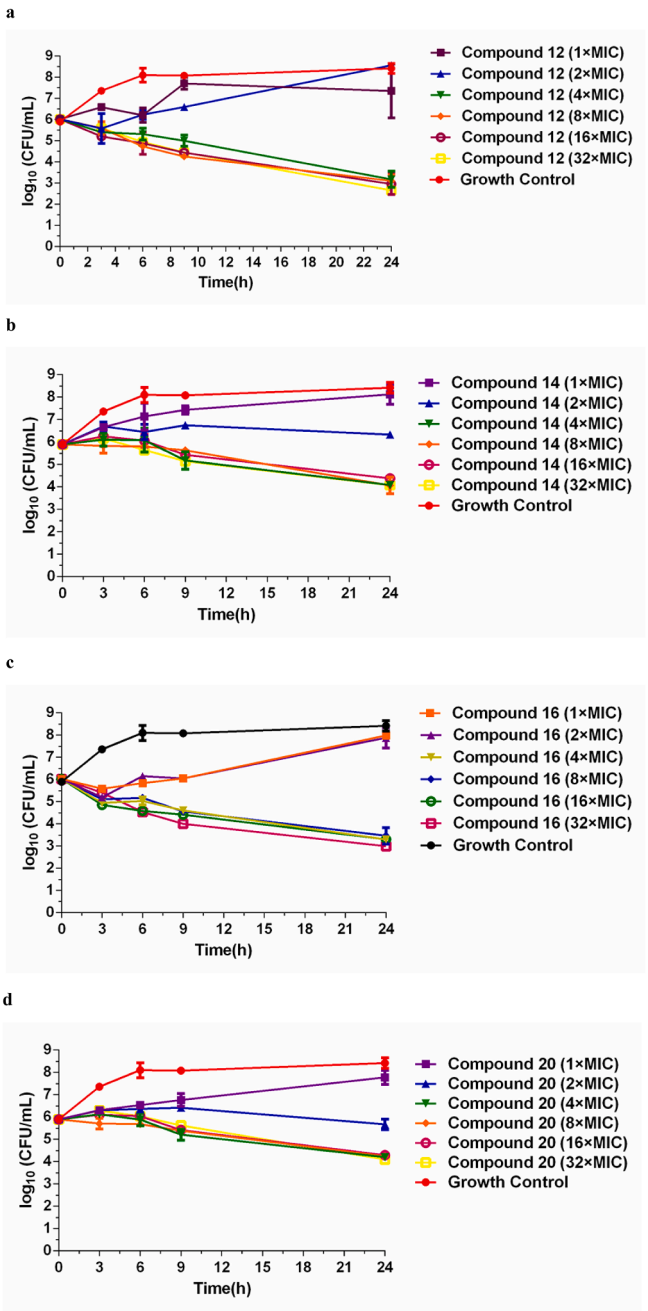

Fig. 2. Time-kill curves for MRSA ATCC 43300 with different concentrations of compounds **12** (a), **14** (b), **16** (c) and **20** (d).

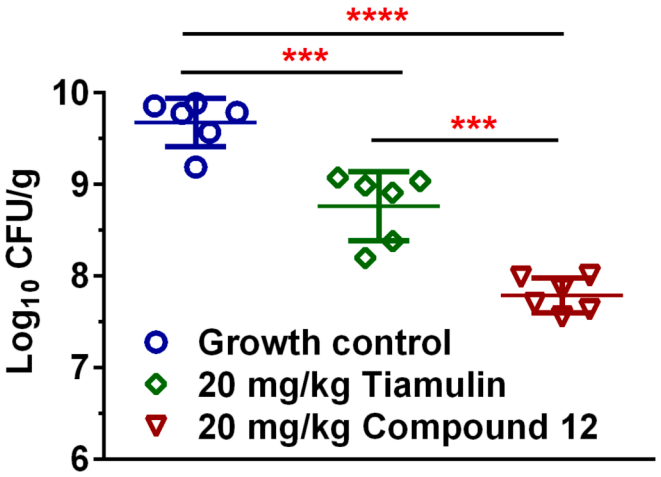

Fig. 3. Efficacy of tiamulin and compound **12** against MRSA ATCC 43300 in murine neutropenic thigh models: circular: growth control; square: tiamulin (20 mg/kg); triangle: compound **12** (20 mg/kg).

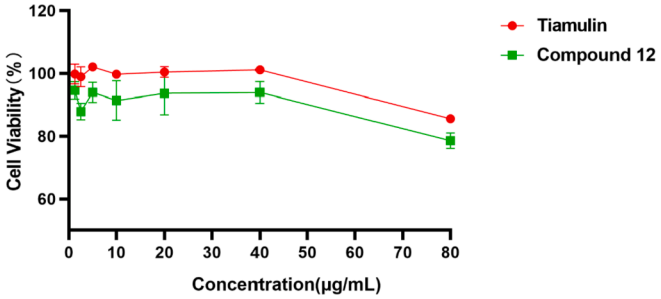

Fig. 4. Cytotoxicity of compound **12** and tiamulin using RAW264.7 cells.

2.7. Molecular docking study

According to the above experimental results, in order to further study the binding of compounds with ribosomes, compound **12** and **20** were selected for molecular docking experiments. The binding free energy of compound **12** with the 50S ribosome was calculated to be −10.7 kcal/mol. As shown in Fig. 7, three strong hydrogen bonds were formed through the interaction of compound **12** with A2530 (O/NH distance: 1.9 Å), A2086 (OH/O distance: 2.0 Å) and U2533 (NH/O distance: 1.9 Å). From Fig. 8, three strong hydrogen bonds were observed through the interaction of compound **20** with G2088 (O/NH distance: 2.2 Å), U2533 (NH/O distance: 1.9 Å) and C2479 (NH/O distance: 2.2 Å). The binding free energy of compound **20** with the ribosome (−11.66 kcal/mol) was slightly lower than compound **12**. This result was consistent with the binding affinity in SPR. One possible reason was that the distance of the hydrogen bond formed between **20** and residues was longer than the

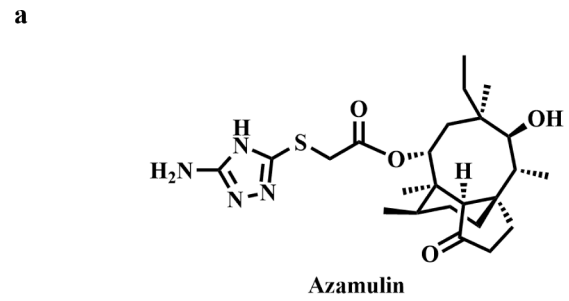

Fig. 5. Effect on liver microsomal CYP450 enzyme activity, (a) structure of azamulin, (b) Inhibition curve of compound **12** on CYP3A4 (Note: Each point in the figure is three parallel averages).

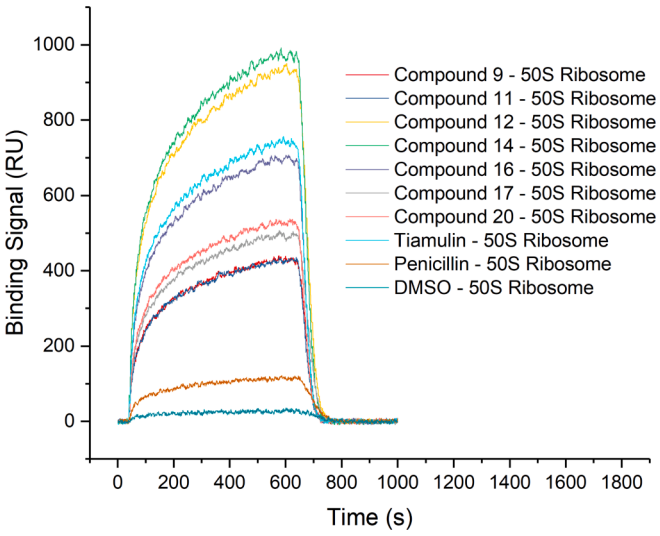

Fig. 6. SPR binding signal curve of seven compounds and controls to 50S ribosome at 3200 nM.

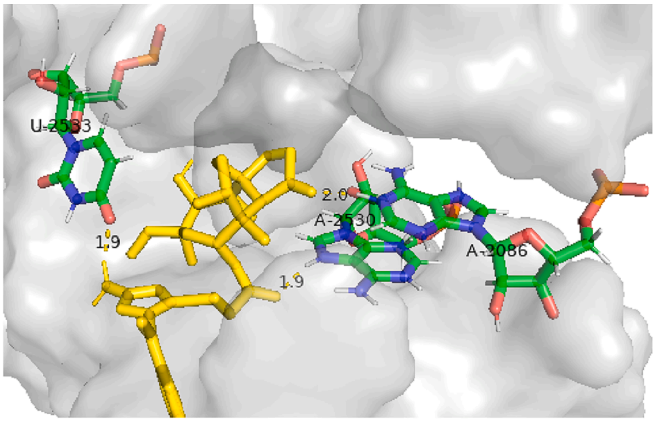

Fig. 7. The simulated docking modes of compounds **12** (yellow) to 5HL7. (For interpretation of the references to colour in this figure legend, the reader is referred to the web version of this article.)

distance of the hydrogen bond formed between **12** and residues.

3. Conclusions

A series of novel pleuromutilin derivatives were designed and synthesized with 1,2,4-triazole as the linker connected to benzoyl chloride analogues in few steps. These derivatives were first evaluated for their *in vitro* antibacterial activity against MRSA (ATCC 43300), *S. aureus* (ATCC 29213), *S. aureus* (AD3) and *S. aureus* (144). Most of the synthesized compounds displayed good antibacterial activity. Compounds **12**, **14**, **16** and **20** showed better antibacterial activity than other compounds and those were selected for the time-kill curve experiment. The results indicated that these derivatives were time-dependent antibacterial agents and had a certain inhibitory effect against MRSA *in vitro*. The *in vivo* antibacterial activity of compound **12** was further evaluated by MRSA infected murine thigh model. The results revealed that compound **12** exhibited superior *in vivo* efficacy than tiamulin. Moreover, compound **12** had no significant inhibitory effect on the proliferation of RAW264.7 cells. CYP450 inhibition experiments showed that inhibitory

Table 2
Binding affinities of compounds and controls between the 50S Ribosome.

Compound	Protein	Avg K_a (1/Ms) [a]	Avg K_d (1/s) [b]	Avg K_D (M) [c]
9	50S Ribosome	1.60×10^{1}	4.30×10^{-3}	2.70×10^{-4}
11	50S Ribosome	1.58×10^{1}	1.39×10^{-4}	8.79×10^{-6}
12	50S Ribosome	4.16×10^{2}	9.14×10^{-2}	2.20×10^{-4}
14	50S Ribosome	5.40×10^{2}	1.20×10^{-2}	2.21×10^{-5}
16	50S Ribosome	9.18×10^{1}	2.04×10^{-5}	2.22×10^{-7}
17	50S Ribosome	2.45×10^{1}	1.48×10^{-1}	6.05×10^{-3}
20	50S Ribosome	3.03×10^{1}	1.50×10^{-5}	4.94×10^{-7}
Tiamulin	50S Ribosome	1.21×10^{2}	3.03×10^{-6}	2.50×10^{-8}
Penicillin	50S Ribosome	2.05	5.20×10^{-1}	2.54×10^{-1}
DMSO	50S Ribosome	2.43	5.80×10^{-1}	2.39×10^{-1}

[a] K_a (association rate constant) indicates the rate of binding of compounds to protein. Avg is the average value of one concentration gradient and the values measured by the parallel test group. [b] K_d (dissociation rate constant) indicates the rate of dissociation between compounds and protein. [c] K_D (equilibrium dissociation constant) = K_d / K_a, it shows the degree of dissociation of compounds and protein in the equilibrium state.

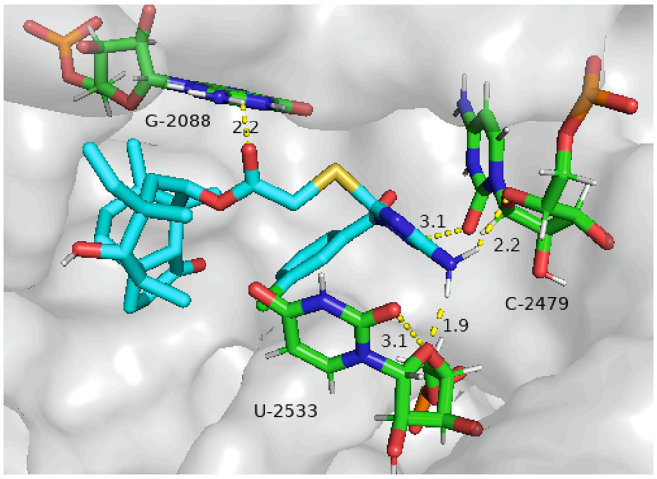

Fig. 8. The simulated docking modes of compounds **20** (cyan) to 5HL7. (For interpretation of the references to colour in this figure legend, the reader is referred to the web version of this article.)

rate of compound **12** on CYP3A4 was lower than that of tiamulin and azamulin. In the SPR study, compounds **11**, **16** and **20** showed strong affinity for the 50S ribosome. Compounds **9**, **12** and **14** showed middle affinity and compound **17** showed weak binding capacity. Subsequently, compounds **12** and **20** were chosen for a molecular docking study. The results showed that the binding free energies were −10.7 kcal/mol and −11.66 kcal/mol, respectively. Three strong hydrogen bonds were formed through the interaction of compound **12** and **20** with residues. According to the above experimental results, compound **12** might serve as a potential agent against MRSA infections for further optimization and discovery.

4. Experimental

4.1. Materials

Pleuromutilin (>90% pure) was purchased from Great Enjoyhood Biochemical Co Ltd (Daying, China). Benzoyl chloride derivatives and 3-amino-5-mercapto-1,2,4-triazole were obtained from J&K Scientific Ltd. The other analytical grade reagents were purchased from Guangzhou Chemical Reagent Factory (Guangzhou, China). Chromatographic purification was carried out on silica gel columns (200–300 mesh, Branch of Qingdao Haiyang Chemical Co., Ltd., Shandong, China). ^{1}H NMR and ^{13}C NMR spectra were measured on Bruker AV-600 spectrometer in Chloroform-*d*. The chemical shift values (δ) are given in parts per million (ppm) downfield from tetramethylsilane, and the coupling constant (*J*) is in Hertz. High-resolution mass spectra were obtained using LCT PXE KE499 with an electro spray ionization (ESI) source.

4.2. Synthesis

The synthetic approaches for the preparation of the intermediates and the general synthesis strategy of novel pleuromutilin derivatives based on compound **1** were illustrated in Scheme 1. Compound 22-(3-amino-1,2,4-triazole-5-yl)-thioacetyl)-22-deoxypleuromutilin (compound **6**) and a variety of benzoyl chloride derivatives were used to prepare pleuromutilin derivatives.

4.2.1. 22-(3-amino-1,2,4-triazole-5-yl)-thioacetyl)-22-deoxypleuromutilin (6)

Compound **7** (1.0 g, 1.88 mmol) was dissolved in acetonitrile (30 mL) and sodium iodide (0.28 g, 1.88 mmol) was added, and the reaction was heated at 70 ℃ for 1 h. 3-amino-5-mercapto-1,2,4-triazole (0.24 g, 2.07 mmol) and K_2CO_3 (0.52 g, 3.76 mmol) were added to the mixture and stirred again for 3 h at 70 ℃. After the reaction was completed, the mixture was extracted with 30 mL of dichloromethane and washed with 30 mL saturated brine 3 times. The organic phase was dried over anhydrous Na_2SO_4 and evaporated in vacuum. The crude product was chromatographed on silica gel (petroleum ether: ethyl acetate = 1:2) to obtain the pure product.

White powder; Yield: 65.8%. ^{1}H NMR (600 MHz, Chloroform-*d*) *δ* 6.38 (1H, dd, *J* = 17.5, 11.0 Hz, H19), 5.72 (1H, d, *J* = 8.5 Hz, H14), 5.22 (1H, dd, *J* = 10.9, 1.5 Hz, H20), 5.16 (1H, dd, *J* = 17.4, 1.5 Hz, H20), 4.87 (2H, s), 3.80 – 3.67 (2H, m, H22), 3.37 (1H, d, *J* = 6.4 Hz, *H*11), 2.33 – 2.01 (5H, m, H2, H4, *H*10, 11-OH), 1.77 – 1.46 (5H, m, H1, H6, H7), 1.46 (3H, s, H15), 1.39 – 1.27 (4H, m, H8, H13), 1.15 (3H, s, H18), 0.89 (3H, d, *J* = 7.0 Hz, H17), 0.70 (3H, d, *J* = 7.1 Hz, H16). ^{13}C NMR (101 MHz, Chloroform-*d*) *δ* 217.16(C3), 168.69(C21), 157.40, 155.55, 139.01(C19), 117.07(C20), 74.58(C11), 70.45(C14), 58.12 (C4), 45.43(C9), 44.51(C13), 44.01(C12), 41.87(C5), 36.66(C6), 36.01 (C10), 34.90(C22), 34.46(*C*2), 30.36(C8), 26.85(C7), 26.65(C18), 24.81 (C1), 16.60(C16), 14.83(C15), 11.49(C17). HR-MS(ESI): Calcd for $C_{24}H_{36}N_4O_4S$(M−H$^+$): 475.2379;Found: 475.2381.

4.2.2. General procedure for the synthesis of compounds 9–28

22-(3-amino-1,2,4-triazole-5-yl)-thioacetyl)-22-deoxypleuromutilin (compound **6**) (1 g, 2.10 mmol) was dissolved in dichloromethane (20 mL). Then added K_2CO_3 (0.58 g, 4.20 mmol) and benzoyl chloride derivatives (3.15 mmol) to the solution and stirred for 6 h at room temperature until reaction was completed. The mixture was washed with dichloromethane (30 mL) and water (50 mL) 3 times. The organic phase was dried over anhydrous Na_2SO_4 and evaporated in vacuum. The crude production was purified by column chromatography (dichloromethane: methanol = 70:1) using silica gel to give the desired compound.

4.2.3. 22-(3-amino-2-benzoyl-1,2,4-triazole-5-yl)-thioacetyl)-22-deoxypleuromutilin (9)

White powder; yield: 32.5%; ^{1}H NMR (600 MHz, Chloroform-*d*) *δ* 8.21 (2H, dd, *J* = 8.1, 1.3 Hz), 7.62 (1H, t, *J* = 7.5, 7.5 Hz), 7.50 (2H, t, *J* = 7.8, 7.8 Hz), 6.71 (2H, s), 6.44 (1H, dd, *J* = 17.4, 11.0 Hz, H19), 5.74 (1H, d, *J* = 8.5 Hz, H14), 5.27 (1H, dd, *J* = 11.0, 1.5 Hz, H20), 5.14 (1H, dd, *J* = 17.4, 1.5 Hz, H20), 3.82 (2H, s, H22), 3.33 (1H, s, *H*11), 2.35 – 1.98 (5H, m, H2, H4, *H*10, 11-OH), 1.76 (1H, dq, *J* = 14.7, 3.2, 3.2, 3.2 Hz, H6), 1.73 – 1.44 (5H, m, H1, H7, H8), 1.42 (3H, s, H15), 1.35 – 1.10 (3H, m, H8, H13), 1.08 (3H, s, H18), 0.87 (3H, d, *J* = 7.0 Hz, H17), 0.69 (3H, d, *J* = 7.0 Hz, H16). ^{13}C NMR (101 MHz, Chloroform-*d*) *δ* 216.88 (C3), 167.45, 167.34 (C21), 160.59, 158.61, 138.98 (C19), 133.39, 131.33, 130.02, 129.13, 128.11, 127.72, 117.10 (C20), 74.57 (C11), 70.00 (C14), 58.14 (C4), 45.43 (C9), 44.57 (C13), 43.89 (C12), 41.86 (C5), 36.72 (C6), 36.00 (C10), 34.43 (C2), 33.91 (C22), 30.40 (C8), 26.83 (C7), 26.39 (C18), 24.82 (C1), 16.66 (C16), 14.84 (C15), 11.41 (C17). HR-MS (ESI): Calcd for $C_{31}H_{40}N_4O_5S$ (M−H$^+$): 579.2641; Found: 579.2659.

4.2.4. 22-(3-amino-2-(2-methyl-benzoyl)-1,2,4-triazole-5-yl)-thioacetyl)-22-deoxypleuromutilin (10)

White powder; yield: 27.3%; ^{1}H NMR (600 MHz, Chloroform-*d*) *δ* 7.55 (1H, dd, *J* = 7.7, 1.3 Hz), 7.43 (1H, td, *J* = 7.6, 7.6, 1.3 Hz), 7.29 (1H, s), 7.26 (1H, d, *J* = 7.7 Hz), 6.75 (2H, s), 6.45 (1H, dd, *J* = 17.4, 11.0 Hz, H19), 5.72 (1H, d, *J* = 8.5 Hz, H14), 5.35 – 5.30 (1H, m, H20), 5.18 (1H, dd, *J* = 17.5, 1.5 Hz, H20), 3.74 (2H, s, H22), 3.35 (1H, d, *J* = 6.4 Hz, *H*11), 2.40 (3H, s, H32), 2.34 – 2.01 (6H, m, H2, H4, *H*10, 11-OH, H13), 1.76 – 1.42 (6H, m, H1, H6, H7, H8), 1.40 (3H, s, H15), 1.38 – 1.23 (2H, m, H8, H13), 1.15 (3H, s, H18), 0.87 (3H, d, *J* = 7.0 Hz, H17), 0.64 (3H, d, *J* = 7.0 Hz, H16). ^{13}C NMR (101 MHz, Chloroform-*d*) *δ* 216.97 (C3), 169.44, 167.34 (C21), 160.52, 158.05, 139.00 (C19), 137.24, 132.04, 131.42, 130.79, 129.20, 125.14, 117.14 (C20), 74.58 (C11), 69.94 (C14), 58.12 (C4), 45.43 (C9), 44.55 (C13), 43.93 (C12), 41.83 (C5), 36.69 (C6), 35.98 (C10), 34.45 (C2), 33.79 (C22), 30.38 (C8), 26.83 (C7), 26.44 (C18), 24.81 (C1), 20.03, 16.65 (C16), 14.82

(C15), 11.44 (C17). HR-MS (ESI): Calcd for $C_{32}H_{42}N_4O_5S$ (M-H$^+$): 593.2798; Found: 593.2557.

4.2.5. 22-(3-amino-2-(3-methyl-benzoyl)-1,2,4-triazole-5-yl)-thioacetyl)-22-deoxypleuromutilin (11)

White powder; yield: 30.7%; ^{1}H NMR (600 MHz, Chloroform-*d*) δ 8.04 – 7.95 (2H, m), 7.39 (2H, dt, J = 15.2, 7.6, 7.6 Hz), 6.75 (2H, s), 6.42 (1H, dd, J = 17.4, 11.0 Hz, H19), 5.73 (1H, d, J = 8.5 Hz, H14), 5.26 (1H, dd, J = 11.0, 1.5 Hz, H20), 5.12 (1H, dd, J = 17.4, 1.6 Hz, H20), 3.81 (2H, s, H22), 3.33 (1H, s, *H*11), 2.44 (3H, s, H32), 2.36 – 1.97 (5H, m, H2, H4, *H*10, 11-OH), 1.82 – 1.44 (6H, m, H1, H6, H7, H8), 1.42 (3H, s, H15), 1.37 – 1.10 (3H, m, H8, H13), 1.07 (3H, s, H18), 0.86 (3H, d, J = 7.0 Hz, H17), 0.69 (3H, d, J = 7.0 Hz, H16). ^{13}C NMR (101 MHz, Chloroform-*d*) δ 216.96 (C3), 167.69, 167.32 (C21), 160.39, 158.67, 138.94 (C19), 137.95, 134.18, 131.66, 131.22, 128.51, 127.96, 117.09 (C20), 74.56 (C11), 69.98 (C14), 58.13 (C4), 45.42 (C9), 44.52 (C13), 43.87 (C12), 41.85 (C5), 36.72 (C6), 35.98 (C10), 34.44 (C2), 33.95 (C22), 30.39 (C8), 26.82 (C7), 26.37 (C18), 24.81 (C1), 21.35, 16.66 (C16), 14.83 (C15), 11.44 (C17). HR-MS (ESI): Calcd for $C_{32}H_{42}N_4O_5S$ (M-H$^+$): 593.2798; Found: 593.2808.

4.2.6. 22-(3-amino-2-(4-methyl-benzoyl)-1,2,4-triazole-5-yl)-thioacetyl)-22-deoxypleuromutilin (12)

White powder; yield: 36.3%; ^{1}H NMR (600 MHz, Chloroform-*d*) δ 8.15 – 8.11 (2H, m), 7.29 (2H, d, J = 8.1 Hz), 6.76 (2H, s), 6.43 (1H, dd, J = 17.4, 11.0 Hz, H19), 5.74 (1H, d, J = 8.5 Hz, H14), 5.26 (1H, dd, J = 11.0, 1.5 Hz, H20), 5.13 (1H, dd, J = 17.4, 1.5 Hz, H20), 3.82 (2H, d, J = 1.1 Hz, H22), 3.36 – 3.31 (1H, m, *H*11), 2.45 (3H, s, H32), 2.32 – 1.98 (5H, m, H2, H4, *H*10, 11-OH), 1.76 – 1.44 (6H, m, H1, H6, H7, H13), 1.43 (3H, s, H15), 1.38 – 1.22 (3H, m, H8, H13), 1.08 (3H, s, H18), 0.87 (3H, d, J = 7.0 Hz, H17), 0.69 (3H, d, J = 7.0 Hz, H16). ^{13}C NMR (101 MHz, Chloroform-*d*) δ 216.98 (C3), 167.31 (C21), 165.09, 160.91, 157.59, 138.99 (C19), 134.11, 134.03, 130.79, 123.83, 117.17 (C20), 116.43, 116.22, 74.57 (C11), 69.97 (C14), 58.12 (C4), 45.42 (C9), 44.50 (C13), 43.92 (C12), 41.84 (C5), 36.70 (C6), 35.98 (C10), 34.45 (C2), 33.85 (C22), 30.38 (C8), 26.82 (C7), 26.40 (C18), 24.81 (C1), 21.05, 16.65 (C16), 14.82 (C15), 11.45 (C17). HR-MS (ESI): Calcd for $C_{32}H_{42}N_4O_5S$ (M-H$^+$): 593.2798; Found: 593.2836.

4.2.7. 22-(3-amino-2-(2-fluoro-benzoyl)-1,2,4-triazole-5-yl)-thioacetyl)-22-deoxypleuromutilin (13)

White powder; yield: 34.2%; ^{1}H NMR (600 MHz, Chloroform-*d*) δ 7.68 (1H, ddd, J = 8.1, 6.7, 1.7 Hz), 7.60 – 7.53 (1H, m), 7.27 – 7.24 (1H, m), 7.21 – 7.16 (1H, m), 6.76 – 6.60 (2H, m), 6.45 (1H, dd, J = 17.4, 11.0 Hz, H19), 5.71 (1H, d, J = 8.5 Hz, H14), 5.35 – 5.26 (1H, m, H20), 5.17 (1H, dd, J = 17.4, 1.5 Hz, H20), 3.75 (2H, s, H22), 3.35 (1H, dd, J = 9.7, 6.4 Hz, *H*11), 2.32 – 2.00 (5H, m, H2, H4, *H*10, 11-OH), 1.79 – 1.42 (7H, m, H1, H6, H7, H8, H13), 1.40 (3H, s, H15), 1.25 (2H, d, J = 16.0 Hz, H8, H13), 1.14 (3H, s, H18), 0.87 (3H, d, J = 7.0 Hz, H17), 0.64 (3H, d, J = 7.0 Hz, H16). ^{13}C NMR (101 MHz, Chloroform-*d*) δ 216.98 (C3), 167.31 (C21), 165.09, 160.91, 157.59, 138.99 (C19), 134.11, 134.03, 130.79, 123.83, 117.17 (C20), 116.43, 116.22, 74.57 (C11), 69.97 (C14), 58.12 (C4), 45.42 (C9), 44.50 (C13), 43.92 (C12), 41.84 (C5), 36.70 (C6), 35.98 (C10), 34.45 (C2), 33.85 (C22), 30.38 (C8), 26.82 (C7), 26.40 (C18), 24.81 (C1), 16.65 (C16), 14.82 (C15), 11.45 (C17). HR-MS (ESI): Calcd for $C_{31}H_{39}FN_4O_5S$ (M-H$^+$): 597.2547; Found: 597.2554.

4.2.8. 22-(3-amino-2-(3-fluoro-benzoyl)-1,2,4-triazole-5-yl)-thioacetyl)-22-deoxypleuromutilin (14)

White powder; yield: 38.6%; ^{1}H NMR (600 MHz, Chloroform-*d*) δ 8.04 (1H, dt, J = 7.8, 1.2, 1.2 Hz), 7.98 (1H, dt, J = 9.6, 2.1, 2.1 Hz), 7.49 (1H, td, J = 8.1, 8.1, 5.5 Hz), 7.33 (1H, td, J = 8.3, 8.3, 2.7 Hz), 6.70 (2H, s), 6.44 (1H, dd, J = 17.4, 11.0 Hz, H19), 5.75 (1H, d, J = 8.5 Hz, H14), 5.27 (1H, dd, J = 11.0, 1.5 Hz, H20), 5.14 (1H, dd, J = 17.4, 1.5 Hz, H20), 3.82 (2H, s, H22), 3.34 (1H, s, *H*11), 2.35 – 1.99 (6H, m, H2, H4, H6, *H*10, 11-OH) , 1.76 – 1.44 (4H, m, H1, H7), 1.43 (3H, s, H15), 1.40 – 1.12 (4H, m, H8, H13), 1.09 (3H, s, H18), 0.87 (3H, dd, J = 7.1, 3.0 Hz, H17), 0.69 (3H, d, J = 7.0 Hz, H16). ^{13}C NMR (101 MHz, Chloroform-*d*) δ 216.96 (C3), 167.28 (C21), 165.95, 163.23, 161.09, 158.64, 138.96 (C19), 129.83, 129.76, 127.18, 120.64, 118.56, 117.12 (C20), 74.55 (C11), 70.04 (C14), 58.12 (C4), 45.42 (C9), 44.55 (C13), 43.87 (C12), 41.85 (C5), 36.71 (C6), 35.98 (C10), 34.44 (C2), 33.89 (C22), 30.39 (C8), 26.82 (C7), 26.34 (C18), 24.81 (C1), 16.68 (C16), 14.81 (C15), 11.44 (C17). HR-MS (ESI): Calcd for $C_{31}H_{39}FN_4O_5S$ (M-H$^+$): 597.2547; Found: 597.2556.

4.2.9. 22-(3-amino-2-(4-fluoro-benzoyl)-1,2,4-triazole-5-yl)-thioacetyl)-22-deoxypleuromutilin (15)

White powder; yield: 34.1%; ^{1}H NMR (600 MHz, Chloroform-*d*) δ 8.36 – 8.27 (2H, m), 7.18 (2H, t, J = 8.7, 8.7 Hz), 6.64 (2H, s), 6.49 – 6.37 (1H, m, H19), 5.74 (1H, d, J = 8.5 Hz, H14), 5.26 (1H, dd, J = 11.0, 1.6 Hz, H20), 5.13 (1H, dd, J = 17.5, 1.7 Hz, H20), 3.81 (2H, d, J = 1.6 Hz, H22), 3.34 (1H, dd, J = 10.6, 6.5 Hz, *H*11), 2.36 – 1.94 (5H, m, H2, H4, *H*10, 11-OH), 1.81 – 1.44 (6H, m, H1, H6, H7, H13), 1.43 (3H, s, H15), 1.37 – 1.10 (3H, m, H8, H13), 1.08 (3H, s, H18), 0.87 (3H, d, J = 7.0 Hz, H17), 0.74 – 0.63 (3H, m, H16). ^{13}C NMR (101 MHz, Chloroform-*d*) δ 216.92 (C3), 167.30 (C21), 167.10, 166.06, 161.14, 158.67, 138.97 (C19), 134.40, 134.30, 127.37, 117.11 (C20), 115.52, 115.31, 74.54 (C11), 70.03 (C14), 58.12 (C4), 45.42 (C9), 44.55 (C13), 43.87 (C12), 41.85 (C5), 36.69 (C6), 35.99 (C10), 34.43 (C2), 33.91 (C22), 30.38 (C8), 26.83 (C7), 26.36 (C18), 24.81 (C1), 16.69 (C16), 14.83 (C15), 11.45 (C17). HR-MS (ESI): Calcd for $C_{31}H_{39}FN_4O_5S$ (M-H$^+$): 597.2547; Found: 597.2572.

4.2.10. 22-(3-amino-2-(4-methoxybenzoyl)-1,2,4-triazole-5-yl)-thioacetyl)-22-deoxypleuromutilin (16)

White powder; yield: 26.9%; ^{1}H NMR (600 MHz, Chloroform-*d*) δ 8.34 – 8.28 (2H, m), 7.00 – 6.96 (2H, m), 6.64 (2H, s), 6.43 (1H, dd, J = 17.4, 11.0 Hz, H19), 5.75 (1H, d, J = 8.5 Hz, H14), 5.26 (1H, dd, J = 11.0, 1.5 Hz, H20), 5.13 (1H, dd, J = 17.4, 1.6 Hz, H20), 3.91 (3H, s, H32), 3.83 (2H, d, J = 2.3 Hz, H22), 3.33 (1H, t, J = 8.1, 8.1 Hz, *H*11), 2.34 – 1.99 (5H, m, H2, H4, *H*10, 11-OH), 1.79 – 1.45 (6H, m, H1, H6, H7, H8), 1.43 (3H, s, H15), 1.36 – 1.24 (3H, m, H8, H13), 1.08 (3H, s, H18), 0.87 (3H, d, J = 7.0 Hz, H17), 0.71 (3H, d, J = 7.1 Hz, H16). ^{13}C NMR (101 MHz, Chloroform-*d*) δ 216.97 (C3), 167.40 (C21), 166.48, 163.84, 160.18, 158.87, 138.97 (C19), 134.08, 129.79, 123.31, 117.09 (C20), 114.42, 113.52, 74.56 (C11), 69.98 (C14), 58.14 (C4), 55.53, 45.43 (C9), 44.54 (C13), 43.87 (C12), 41.86 (C5), 36.72 (C6), 35.99 (C10), 34.44 (C2), 33.96 (C22), 30.39 (C8), 26.83 (C7), 26.36 (C18), 24.81 (C1), 16.70 (C16), 14.84 (C15), 11.45 (C17). HR-MS (ESI): Calcd for $C_{32}H_{42}N_4O_6S$ (M-H$^+$): 609.2747; Found: 609.2770.

4.2.11. 22-(3-amino-2-(3-methoxybenzoyl)-1,2,4-triazole-5-yl)-thioacetyl)-22-deoxypleuromutilin (17)

White powder; yield: 27.6%; ^{1}H NMR (600 MHz, Chloroform-*d*) δ 7.82 (1H, dt, J = 7.7, 1.4, 1.4 Hz), 7.74 (1H, p, J = 1.1, 1.1, 1.1, 1.1 Hz), 7.40 (1H, t, J = 8.0, 8.0 Hz), 7.16 (1H, dd, J = 8.2, 2.7 Hz), 6.62 (2H, s), 6.42 (1H, dd, J = 17.5, 11.0 Hz, H19), 5.73 (1H, d, J = 8.5 Hz, H14), 5.27 (1H, dd, J = 11.0, 1.5 Hz, H20), 5.12 (1H, dt, J = 17.4, 1.4, 1.4 Hz, H20), 3.88 (3H, d, J = 0.9 Hz, H32), 3.82 (2H, s, H22), 3.33 (1H, dd, J = 10.6, 6.5 Hz, H11), 2.36 – 1.92 (5H, m, H2, H4, H10, 11-OH), 1.76 – 1.44 (7H, m, H1, H6, H7, H8, H13), 1.42 (3H, s, H15), 1.36 – 1.11 (2H, m, H8, H13), 1.07 (3H, s, H18), 0.87 (3H, d, J = 7.0 Hz, H17), 0.69 (3H, d, J = 6.9 Hz, H16). ^{13}C NMR (101 MHz, Chloroform-*d*) δ 216.97 (C3), 167.31 (C21), 167.20, 160.67, 159.15, 158.63, 138.93 (C19), 132.34, 129.15, 123.90, 119.91, 117.12 (C20), 115.90, 74.56 (C11), 70.00 (C14), 58.12 (C4), 55.48, 45.42 (C9), 44.49 (C13), 43.86 (C12), 41.84 (C5), 36.71 (C6), 35.98 (C10), 34.45 (C2), 33.95 (C22), 30.39 (C8), 26.82 (C7), 26.35 (C18), 24.81 (C1), 16.68 (C16), 14.80 (C15), 11.45 (C17). HR-MS (ESI): Calcd for $C_{32}H_{42}N_4O_6S$ (M-H$^+$): 609.2747; Found: 609.2731.

4.2.12. 22-(3-amino-2-(2-methoxybenzoyl)-1,2,4-triazole-5-yl)-thioacetyl)-22-deoxypleuromutilin (18)

White powder; yield: 21.0%; ^{1}H NMR (600 MHz, Chloroform-*d*) δ 7.53 – 7.45 (2H, m), 7.07 – 6.97 (2H, m), 6.65 – 6.53 (2H, m), 6.45 (1H, ddd, J = 17.5, 11.0, 1.8 Hz, H19), 5.71 (1H, d, J = 8.4 Hz, H14), 5.36 – 5.29 (1H, m, H20), 5.18 (1H, dt, J = 17.4, 1.8, 1.8 Hz, H20), 3.85 (3H, d, J = 1.6 Hz, H32), 3.73 (2H, s, H22), 3.35 (1H, dd, J = 10.4, 6.4 Hz, H11), 2.36 – 1.95 (5H, m, H2, H4, H10, 11-OH), 1.80 –1.44 (7H, m, H1, H6, H7, H8, H13), 1.39 (3H, d, J = 1.6 Hz, H15), 1.37 – 1.20 (2H, m, H8, H13), 1.14 (3H, d, J = 1.5 Hz, H18), 0.87 (3H, d, J = 6.9 Hz, H17), 0.64 (3H, dd, J = 7.0, 1.8 Hz, H16). ^{13}C NMR (101 MHz, Chloroform-*d*) δ 216.98 (C3), 167.79, 167.42 (C21), 160.12, 157.63, 157.49, 139.00 (C19), 133.06, 129.84, 122.23, 120.07, 117.16 (C20), 111.65, 74.58 (C11), 69.90 (C14), 58.13 (C4), 55.91, 45.43 (C9), 44.52 (C13), 43.93 (C12), 41.84 (C5), 36.71 (C6), 35.98 (C10), 34.45 (C2), 33.86 (C22), 30.39 (C8), 26.84 (C7), 26.42 (C18), 24.81 (C1), 16.66 (C16), 14.82 (C15), 11.45 (C17). HR-MS (ESI): Calcd for $C_{32}H_{42}N_4O_6S$ (M-H$^+$): 609.2747; Found: 609.2753.

4.2.13. 22-(3-amino-2-(2-chloro-benzoyl)-1,2,4-triazole-5-yl)-thioacetyl)-22-deoxypleuromutilin (19)

White powder; yield: 25.1%; ^{1}H NMR (600 MHz, Chloroform-*d*) δ 7.53 (1H, dt, J = 7.6, 1.1, 1.1 Hz), 7.50 – 7.44 (2H, m), 7.37 (1H, dt, J = 7.6, 4.4, 4.4 Hz), 6.58 (s, 2H), 6.45 (1H, dd, J = 17.4, 11.0 Hz, H19), 5.72 (1H, d, J = 8.4 Hz, H14), 5.33 (1H, dd, J = 11.0, 1.5 Hz, H20), 5.19 (1H, dd, J = 17.4, 1.6 Hz, H20), 3.73 (2H, s, H22), 3.35 (1H, s, *H*11), 2.35 – 1.95 (5H, m, H2, H4, *H*10, 11-OH), 1.76 – 1.42 (8H, m, H1, H6, H7, H8, H13), 1.40 (3H, s, H15), 1.38 – 1.23 (1H, m, H8), 1.16 (3H, s, H18), 0.87 (3H, d, J = 7.0 Hz, H17), 0.64 (3H, d, J = 7.0 Hz, H16). ^{13}C NMR (101 MHz, Chloroform-*d*) δ 216.95 (C3), 167.29 (C21), 166.65, 161.15, 157.55, 138.99 (C19), 132.43, 132.19, 131.88, 130.02, 129.60, 126.38, 117.19 (C20), 74.57 (C11), 69.97 (C14), 58.12 (C4), 45.43 (C9), 44.55 (C13), 43.94 (C12), 41.84 (C5), 36.69 (C6), 35.98 (C10), 34.45 (C2), 33.85 (C22), 30.39 (C8), 26.83 (C7), 26.41 (C18), 24.81 (C1), 16.69 (C16), 14.83 (C15), 11.45 (C17). HR-MS (ESI): Calcd for $C_{31}H_{39}ClN_4O_5S$ (M-H$^+$): 613.2252; Found: 613.2225.

4.2.14. 22-(3-amino-2-(3-chloro-benzoyl)-1,2,4-triazole-5-yl)-thioacetyl)-22-deoxypleuromutilin (20)

White powder; yield: 28.4%; ^{1}H NMR (600 MHz, Chloroform-*d*) δ 8.21 (t, J = 1.9, 1.9 Hz, 1H), 8.12 (dt, J = 7.9, 1.2, 1.2 Hz, 1H), 7.59 (dd, J = 8.0, 2.1 Hz, 1H), 7.44 (t, J = 7.9, 7.9 Hz, 1H), 6.86 (s, 2H), 6.42 (1H, dd, J = 17.4, 11.0 Hz, H19), 5.73 (1H, d, J = 8.5 Hz, H14), 5.26 (1H, dd, J = 10.9, 1.5 Hz, H20), 5.12 (1H, dd, J = 17.4, 1.5 Hz, H20), 3.81 (2H, s, H22), 3.33 (1H, d, J = 6.4 Hz, *H*11), 2.32 – 1.98 (5H, m, H2, H4, *H*10, 11-OH), 1.75 – 1.43 (5H, m, H1, H6, H7), 1.42 (3H, s, H15), 1.36 – 1.13 (4H, m, H8, H13), 1.07 (3H, s, H18), 0.86 (3H, d, J = 7.0 Hz, H17), 0.68 (3H, d, J = 7.1 Hz, H16). ^{13}C NMR (101 MHz, Chloroform-*d*) δ 217.01 (C3), 167.23 (C21), 165.94, 161.03, 158.77, 138.94 (C19), 134.27, 133.36, 132.88, 131.26, 129.47, 129.41, 117.09 (C20), 74.55 (C11), 70.06 (C14), 58.11 (C4), 45.42 (C9), 44.54 (C13), 43.86 (C12), 41.84 (C5), 36.69 (C6), 35.97 (C10), 34.44 (C2), 33.91 (C22), 30.37 (C8), 26.81 (C7), 26.38 (C18), 24.81 (C1), 16.67 (C16), 14.83 (C15), 11.45 (C17). HR-MS (ESI): Calcd for $C_{31}H_{39}ClN_4O_5S$ (M-H$^+$): 613.2252; Found: 613.2223.

4.2.15. 22-(3-amino-2-(4-chloro-benzoyl)-1,2,4-triazole-5-yl)-thioacetyl)-22-deoxypleuromutilin (21)

White powder; yield: 23.2%; ^{1}H NMR (600 MHz, Chloroform-*d*) δ 8.20 (2H, dt, J = 9.0, 2.7, 2.7 Hz), 7.47 (2H, dt, J = 8.9, 2.7, 2.7 Hz), 6.80 (2H, s), 6.42 (1H, ddt, J = 16.8, 10.9, 2.8, 2.8 Hz, H19), 5.73 (1H, dd, J = 8.7, 2.8 Hz, H14), 5.27 – 5.21 (1H, m, H20), 5.12 (1H, ddt, J = 17.5, 4.1, 1.9, 1.9 Hz, H20), 3.80 (2H, d, J = 2.6 Hz, H22), 3.40 – 3.25 (1H, m, *H*11), 2.25 – 1.91 (5H, m, H2, H4, H10, 11-OH), 1.75 – 1.48 (6H, m, H1, H6, H7, H13), 1.43 (3H, t, J = 2.8, 2.8 Hz, H15), 1.40 – 1.11 (3H, m, H8, H13), 1.08 (3H, d, J = 2.8 Hz, H18), 0.86 (3H, dt, J = 6.1, 2.8, 2.8 Hz, H17), 0.69 (3H, dt, J = 6.0, 2.8, 2.8 Hz, H16). ^{13}C NMR (101 MHz, Chloroform-*d*) δ 216.91 (C3), 167.26 (C21), 166.24, 160.88, 158.71, 140.02, 138.96 (C19), 132.87, 132.36, 129.57, 128.51, 128.14, 117.10 (C20), 74.53 (C11), 70.07 (C14), 58.11 (C4), 45.42 (C9), 44.56 (C13), 43.87 (C12), 41.85 (C5), 36.69 (C6), 35.99 (C10), 34.43 (C2), 33.89 (C22), 30.37 (C8), 26.83 (C7), 26.38 (C18), 24.81 (C1), 16.69 (C16), 14.83 (C15), 11.44 (C17). HR-MS (ESI): Calcd for $C_{31}H_{39}ClN_4O_5S$ (M-H$^+$): 613.2252; Found: 613.2244.

4.2.16. 22-(3-amino-2-(2-(trifluoromethyl)benzoyl)-1,2,4-triazole-5-yl)-thioacetyl)-22-deoxypleuromutilin (22)

White powder; yield: 40.6%; ^{1}H NMR (600 MHz, Chloroform-*d*) δ 7.80 – 7.75 (1H, m), 7.70 – 7.64 (2H, m), 7.61 – 7.55 (1H, m), 6.68 (2H, s), 6.45 (1H, dd, J = 17.5, 11.0 Hz, H19), 5.71 (1H, d, J = 8.5 Hz, H14), 5.32 (1H, dd, J = 11.0, 1.5 Hz, H20), 5.18 (1H, dd, J = 17.5, 1.5 Hz, H20), 3.70 (2H, s, H22), 3.36 (1H, d, J = 6.4 Hz, H11), 2.31 – 1.99 (5H, m, H2, H4, *H*10, 11-OH), 1.76 – 1.42 (6H, m, H1, H6, H7, H13), 1.39 (3H, s, H15), 1.34 – 1.25(2H, m, H8, H13), 1.15 (3H, s, H18), 1.11 (1H, dd, J = 14.1, 4.4 Hz, H13), 0.88 (3H, d, J = 7.0 Hz, H17), 0.63 (3H, d, J = 7.0 Hz, H16). ^{13}C NMR (101 MHz, Chloroform-*d*) δ 216.86 (C3), 167.20 (C21), 161.23, 157.65, 139.03 (C19), 131.37, 131.24, 131.02, 128.79, 128.24, 128.02, 126.70, 124.20, 117.12 (C20), 74.59 (C11), 70.02 (C14), 58.12 (C4), 45.43 (C9), 44.58 (C13), 43.95 (C12), 41.85 (C5), 36.68 (C6), 36.00 (C10), 34.44 (C2), 33.75 (C22), 30.39 (C8), 26.83 (C7), 26.41 (C18), 24.82 (C1), 16.62 (C16), 14.78 (C15), 11.41 (C17). HR-MS (ESI): Calcd for $C_{32}H_{39}F_3N_4O_5S$ (M-H$^+$): 647.2515; Found: 647.2514.

4.2.17. 22-(3-amino-2-(4-(trifluoromethyl)benzoyl)-1,2,4-triazole-5-yl)-thioacetyl)-22-deoxypleuromutilin (23)

White powder; yield: 37.4%; ^{1}H NMR (600 MHz, Chloroform-*d*) δ 8.35 – 8.30 (2H, m), 7.77 (2H, d, J = 8.3 Hz), 6.79 (2H, s), 6.44 (1H, dd, J = 17.4, 11.0 Hz, H19), 5.74 (1H, d, J = 8.5 Hz, H14), 5.26 (1H, dd, J = 11.0, 1.5 Hz, H20), 5.13 (1H, dd, J = 17.4, 1.6 Hz, H20), 3.80 (2H, d, J = 2.4 Hz, H22), 3.34 (1H, d, J = 6.4 Hz, *H*11), 2.32 – 1.96 (5H, m, H2, H4, *H*10, 11-OH), 1.76 – 1.43 (6H, m, H1, H6, H7, H13), 1.42 (3H, s, H15), 1.35 – 1.14 (3H, m, H8, H13), 1.09 (3H, s, H18), 0.87 (3H, d, J = 7.0 Hz, H17), 0.68 (3H, d, J = 7.1 Hz, H16). ^{13}C NMR (101 MHz, Chloroform-*d*) δ 216.78 (C3), 167.20 (C21), 166.18, 161.29, 158.61, 139.01 (C19), 134.74, 134.50, 131.64, 130.37, 125.12, 124.36, 122.55, 117.07 (C20), 74.55 (C11), 70.13 (C14), 58.11 (C4), 45.42 (C9), 44.63 (C13), 43.89 (C12), 41.87 (C5), 36.69 (C6), 36.01 (C10), 34.42 (C2), 33.84 (C22), 30.38 (C8), 26.84 (C7), 26.39 (C18), 24.81 (C1), 16.67 (C16), 14.80 (C15), 11.40 (C17). HR-MS (ESI): Calcd for $C_{32}H_{39}F_3N_4O_5S$ (M-H$^+$): 647.2515; Found: 647.2507.

4.2.18. 22-(3-amino-2-(3,5-dichlorobenzoyl)-1,2,4-triazole-5-yl)-thioacetyl)-22-deoxypleuromutilin (24)

White powder; yield: 35.8%; ^{1}H NMR (600 MHz, Chloroform-*d*) δ 8.13 (2H, d, J = 1.9 Hz), 7.60 (1H, t, J = 1.9, 1.9 Hz), 6.72 (2H, s), 6.43 (1H, dd, J = 17.4, 11.0 Hz, H19), 5.74 (1H, d, J = 8.5 Hz, H14), 5.26 (1H, dd, J = 11.0, 1.5 Hz, H20), 5.13 (1H, dd, J = 17.4, 1.6 Hz, H20), 3.81 (2H, d, J = 0.5 Hz, H22), 3.34 (1H, d, J = 6.3 Hz, *H*11), 2.32 – 1.97 (5H, m, H2, H4, *H*10, 11-OH), 1.76 – 1.44 (5H, m, H1, H7, H13), 1.43 (3H, s, H15), 1.34 – 1.11 (4H, m, H6,H8, H13), 1.09 (3H, s, H18), 0.87 (3H, d, J = 7.1 Hz, H17), 0.69 (3H, d, J = 7.1 Hz, H16). ^{13}C NMR (101 MHz, Chloroform-*d*) δ 216.86 (C3), 167.11 (C21), 164.62, 161.65, 158.56, 139.01 (C19), 135.03, 133.82, 133.14, 129.64, 117.05 (C20), 74.56 (C11), 70.12 (C14), 58.43, 58.13 (C4), 45.43 (C9), 44.61 (C13), 43.90 (C12), 41.87 (C5), 36.71 (C6), 36.01 (C10), 34.44 (C2), 33.94 (C22), 30.40 (C8), 26.83 (C7), 26.38 (C18), 24.82 (C1), 18.42, 16.66 (C16), 14.82 (C15), 11.40 (C17). HR-MS (ESI): Calcd for $C_{31}H_{38}Cl_2N_4O_5S$ (M-H$^+$): 647.1862; Found: 647.1877.

4.2.19. 22-(3-amino-2-(perfluorobenzoyl)-1,2,4-triazole-5-yl)-thioacetyl)-22-deoxypleuromutilin (25)

White powder; yield: 32.2%; ^{1}H NMR (600 MHz, Chloroform-*d*) δ 6.65 (2H, s), 6.46 (1H, dd, J = 17.4, 11.0 Hz, H19), 5.72 (1H, d, J = 8.5 Hz, H14), 5.33 (1H, dd, J = 11.0, 1.5 Hz, H20), 5.19 (1H, dd, J = 17.4, 1.6 Hz, H20), 3.72 (2H, d, J = 7.0 Hz, H22), 3.36 (1H, d, J = 6.5 Hz, *H*11), 2.33 – 2.01 (6H, m, H1,H2, H4, *H*10, 11-OH), 2.12 – 2.01 (2H, m), 1.77 – 1.61 (3H, m, H1, H7), 1.56 – 1.43 (3H, m, H6, H8, H13), 1.42 (3H, s, H15), 1.40 – 1.18 (2H, m, H8, H13), 1.16 (3H, s, H18), 0.88 (3H, d, J = 7.0 Hz, H17), 0.66 (3H, d, J = 7.1 Hz, H16). ^{13}C NMR (101 MHz, Chloroform-*d*) δ 216.76 (C3), 173.62, 171.10, 166.95 (C21), 162.71, 160.00, 157.70, 157.07, 139.01 (C19), 117.07 (C20), 74.57 (C11), 70.24 (C14), 60.36, 58.10 (C4), 45.43 (C9), 44.65 (C13), 43.96 (C12), 41.86 (C5), 36.66 (C6), 36.00 (C10), 34.42 (C2), 33.83 (C22), 30.39 (C8), 26.80 (C7), 26.35 (C18), 24.80 (C1), 21.00, 16.56 (C16), 14.70 (C15), 14.18, 11.39 (C17). HR-MS (ESI): Calcd for $C_{31}H_{35}F_5N_4O_5S$ (M-H$^+$): 669.2170; Found: 669.2197.

4.2.20. 22-(3-amino-2-(4-(trifluoromethoxy)benzoyl)-1,2,4-triazole-5-yl)-thioacetyl)-22-deoxypleuromutilin (26)

White powder; yield: 36.7%; ^{1}H NMR (600 MHz, Chloroform-*d*) δ 8.37 – 8.32 (2H, m), 7.33 (2H, dq, J = 9.0, 1.0, 1.0, 1.0 Hz), 6.70 (2H, s), 6.44 (1H, dd, J = 17.4, 11.0 Hz, H19), 5.75 (1H, d, J = 8.5 Hz, H14), 5.26 (1H, dd, J = 11.0, 1.5 Hz, H20), 5.14 (1H, dd, J = 17.4, 1.6 Hz, H20), 3.85 – 3.77 (2H, m, H22), 3.34 (1H, d, J = 6.5 Hz, *H*11), 2.34 – 1.97 (5H, m, H2, H4, *H*10, 11-OH), 1.79 – 1.44 (6H, m, H1, H6, H7, H13), 1.43 (3H, s, H15), 1.38 – 1.10 (3H, m, H8, H13), 1.09 (3H, s, H18), 0.87 (3H, d, J = 7.1 Hz, H17), 0.70 (3H, d, J = 7.1 Hz, H16). ^{13}C NMR (101 MHz, Chloroform-*d*) δ 216.76 (C3), 167.24 (C21), 165.88, 164.49, 163.07, 161.02, 158.65, 152.83, 139.02 (C19), 138.73, 133.67, 129.39, 119.79, 117.05 (C20), 74.56 (C11), 70.09 (C14), 58.12 (C4), 45.43 (C9), 44.64 (C13), 43.89 (C12), 41.87 (C5), 36.70 (C6), 36.02 (C10), 34.42 (C2), 33.88 (C22), 30.39 (C8), 26.84 (C7), 26.37 (C18), 24.82 (C1), 16.66 (C16), 14.79 (C15), 11.40 (C17). HR-MS (ESI): Calcd for $C_{32}H_{39}F_3N_4O_6S$ (M-H$^+$): 663.2464; Found: 663.2471.

4.2.21. 22-(3-amino-2-(2-chloro-4-fluorobenzoyl)-1,2,4-triazole-5-yl)-thioacetyl)-22-deoxypleuromutilin (27)

White powder; yield: 34.1%; ^{1}H NMR (600 MHz, Chloroform-*d*) δ 7.58 (1H, dd, J = 8.7, 5.8 Hz), 7.23 (1H, dd, J = 8.4, 2.4 Hz), 7.13 – 7.07 (1H, m), 6.60 (2H, s), 6.45 (1H, dd, J = 17.4, 11.0 Hz, H19), 5.72 (1H, d, J = 8.5 Hz, H14), 5.33 (1H, dd, J = 11.0, 1.5 Hz, H20), 5.19 (1H, dd, J = 17.4, 1.6 Hz, H20), 3.73 (2H, s, H22), 3.36 (1H, d, J = 6.5 Hz, *H*11), 2.34 – 2.03 (5H, m, H2, H4, *H*10, 11-OH), 1.81 – 1.44 (6H, m, H1, H6, H7, H13), 1.41 (3H, s, H15), 1.38 – 1.24 (3H, m, H8, H13), 1.16 (3H, s, H18), 0.88 (3H, d, J = 7.1 Hz, H17), 0.66 (3H, d, J = 7.1 Hz, H16). ^{13}C NMR (101 MHz, Chloroform-*d*) δ 216.78 (C3), 167.20 (C21), 165.70, 161.35, 157.59, 139.05 (C19), 133.90, 131.66, 117.88, 117.72, 117.13 (C20), 114.04, 113.89, 74.58 (C11), 70.06 (C14), 58.12 (C4), 45.43 (C9), 44.62 (C13), 43.97 (C12), 41.86 (C5), 36.69 (C6), 36.02 (C10), 34.43 (C2), 33.84 (C22), 30.39 (C8), 26.85 (C7), 26.46 (C18), 24.82 (C1), 16.66 (C16), 14.81 (C15), 11.41 (C17). HR-MS (ESI): Calcd for $C_{31}H_{38}ClFN_4O_5S$ (M-H$^+$): 631.2157; Found: 631.2177.

4.2.22. 22-(3-amino-2-(2-chloro-6-fluorobenzoyl)-1,2,4-triazole-5-yl)-thioacetyl)-22-deoxypleuromutilin (28)

White powder; yield: 36.5%; ^{1}H NMR (600 MHz, Chloroform-*d*) δ 7.44 (1H, td, J = 8.3, 8.3, 5.9 Hz), 7.29 (1H, p, J = 0.8, 0.8, 0.8, 0.8 Hz), 7.11 (1H, tdd, J = 8.5, 8.5, 2.9, 0.9 Hz), 6.66 – 6.59 (2H, m), 6.45 (1H, ddd, J = 17.5, 11.1, 1.4 Hz, H19), 5.71 (1H, d, J = 8.5 Hz, H14), 5.33 (1H, dt, J = 11.0, 1.6, 1.6 Hz, H20), 5.21 – 5.17 (1H, m, H20), 3.72 (2H, s, H22), 3.40 – 3.33 (1H, m, *H*11), 2.34 – 1.99 (5H, m, H2, H4, *H*10, 11-OH), 1.79 – 1.42 (6H, m, H1, H6, H7, H13), 1.40 (3H, s, H15), 1.37 – 1.23 (3H, m, H8, H13), 1.16 (3H, d, J = 1.8 Hz, H18), 0.88 (3H, d, J = 7.0 Hz, H17), 0.65 (3H, dd, J = 7.1, 3.7 Hz, H16). ^{13}C NMR (101 MHz, Chloroform-*d*) δ 216.82 (C3), 167.20 (C21), 162.62, 161.79, 160.09, 158.41, 157.17, 139.04 (C19), 132.32, 132.16, 125.42, 117.12 (C20), 114.25, 74.60 (C11), 70.05 (C14), 58.13 (C4), 45.44 (C9), 44.61 (C13), 43.97 (C12), 41.87 (C5), 36.70 (C6), 36.00 (C10), 34.44 (C2), 33.85 (C22), 30.40 (C8), 26.84 (C7), 26.43 (C18), 24.82 (C1), 16.67 (C16), 14.80 (C15), 11.42 (C17). HR-MS (ESI): Calcd for $C_{31}H_{38}ClFN_4O_5S$ (M-H$^+$): 631.2157; Found: 631.2166.

4.3. In vitro efficacy of pleuromutilin derivatives

4.3.1. Minimal inhibitory concentration (MIC) testing

The MIC values of all synthesized pleuromutilin derivatives against MRSA (ATCC 43300), *S. aureus* (ATCC 29213), *S. aureus* (AD3) and *S. aureus* (144) were determined by using tiamulin as positive control. The MIC values were determined by broth dilution in accordance with the Clinical and Laboratory Standards Institute (CLSI). Stock solutions of these compounds were prepared in 95% deionized water, 2.5% Dimethyl sulfoxide (DMSO) and 2.5% Tween 80 at the concentration of 1280 μg/mL. The working solutions (640 μg/mL) were obtained by diluting stock solutions in sterile Mueller Hinton (MH) broth.

The drug susceptibility testing was performed in 96-well plate. 180 μL MH broth was added to the first well of rows 1 to 6 of a 96-well plate, and 100 μL MH broth was added to the other wells. 20 μL of the compound working solutions (640 μg/mL) was added to the first hole of 1–6 rows and well mixed. Then 100 μL of the mixture from column 1 was inhaled to the wells in column 2, well mixed. Similar operations were repeated until the wells in column 12 were filled. 100 μL mixture from the wells in column 12 was discarded. 100 μL of the bacteria solution was added to the wells in rows 1 to 7 in columns 1 to 12, well mixed. Three repetitions were made for each bacterial and each tested compound. Sterile MH broth as negative control, bacterial solution as positive control. The tested concentration ranges were 0.03125–64 μg/mL. All 96 well plates were cultured at 37 ℃ for 24 h, and the results were observed. The MIC value refers to the lowest concentration in the sample to inhibit the visible growth of the tested bacteria. The control drugs tiamulin was tested under the same conditions.

4.3.2. Constant concentration time-kill curves

The time-kill curve experiment of *in vitro* kinetic model was used to study the antibacterial effect of constant drug concentration on MRSA *in vitro*. The experiments were performed in triplicate according our previously work.[14] In this experiment, MRSA was cultured in MH broth at 37 ℃ for 4.5 h, then diluted to 1 × 10^6 CFU/mL. The concentrations of tested compounds were configured as 1 × MIC, 2 × MIC, 4 × MIC, 8 × MIC, 16 × MIC and 32 × MIC, and the growth control only containing 0.9% saline. All bacterial solutions were cultured in 37 ℃ constant temperature shaking incubator, sampling times included 0, 3, 6, 9 and 24 h. The sample (100 μL) was extracted from the solution at each designated time point and diluted 10-fold continuously in saline. Then 25 μL of the dilutions were plated onto the MH agar plates. The total number of bacteria CFU/mL on the culture plates were determined after 24 h of incubation at 37 ℃. The time-kill curve was drawn by plotting log CFU/mL against time.

4.4. Neutropenic murine thigh infection model

The animal experiments were approved by the Animal Research Committees of the South China Agriculture University (SYXK2019-0136) and carried out in strict accordance with the recommendations in the Guide for the Care and Use of Laboratory Animals of the National Institutes of Health. Randomly select 9 female ICR / Swiss mice at 6 weeks of age, weighing 22–28 g, without specific pathogens, were intraperitoneally injected with 150 mg/kg cyclophosphamide (Mead Johnson Pharmaceuticals, Evansville, IN) 4 days before infection, and intraperitoneally injected with 100 mg/kg cyclophosphamide 1 day before infection, resulting in a decrease of neutrophil(<0.1 × 10^9/L). A single MRSA colony was inoculated into a tube containing MH broth for

culture. Mice were anesthetized with ether, and then 0.1 mL warm MH broth (about 10^7 CFU/mL) was injected into each thigh to produce a thigh infection model caused by MRSA.

Two hours after the growth of bacteria in the thigh of mice, the mice were divided into 3 groups, 3 in each group, and injected with saline, compound **12** (20 mg/kg) and tiamulin (20 mg/kg) intravenously. The first group of mice was injected with normal saline as control. Three mice in each group were euthanized 24 h after injection. After death, six thighs of each group were taken out and homogenized (Polytron tissue homogenizer, Kinematica, Lucerne, Switzerland) in 3 mL iced saline. Each sample solution was diluted 10-fold in saline, and plated onto MH agar plates. After incubating these plates at 37 ℃ for 24 h, the colonies (CFU/mL) were counted.

4.5. Cytotoxicity assay

MTT assay was used to assess cell viability as described in the references.[15] The cell line was RAW 264.7 cells in this experiment. 100 μL DMEM containing RAW 264.7 cells at a density of 1.0×10^5 cells per well were added into 96-well plates and incubated at 37 ℃ for 24 h. Then medium were replaced with 100 μL test compounds of serial concentrations of 1.25, 2.5, 5, 10, 20, 40 and 80 μg/mL and incubated at 37 ℃ for 16 h. After that, all reagents in cells were removed and 100 μL of 0.5 mg/mL MTT per well was added, followed by incubation at 37 ℃ for 4 h. The media were removed and cells were dissolved in 150 μL DMSO. DMSO was used as the positive control and wells without cells were left as the negative control. The absorbance of each well was measured at 570 nm by a spectrophotometer. The cell viability was calculated by the formula: cell viability% = $(OD_{sample} - OD_{blank}/ OD_{control} - OD_{blank}) \times 100$. The assay was repeated at least three times.

4.6. Effect on human liver microsomal CYP450 enzyme activity

Inhibition effect of compound **12** on CYP3A4 were evaluated according previous work.[21] Each well of 96-well plate contained 40 μL of human liver microsomes (final concentration of human liver microsomes is 0.2 mg/mL), 20 μL of compound **12** and 20 μL of probe substrates (final concentration of testosterone is 20 μmol/L) in 0.1 M Tris (pH 7.4). The final concentrations of compound **12** were 2.5, 5, 10, 20, 40, and 80 μM, respectively. The plate was incubated at 37 ℃ for 5 min, the reaction started with the addition of 20 μL NADPH (final concentration is 1 mmol/L). After incubation at 37 ℃ for 5 min, 100 μL acetonitrile with 50 nM loratadine as the internal standard was added to terminate the reaction. The mixtures were centrifuged and supernatants were analyzed by LC-MS/MS.

4.7. S. aureus growth and ribosome purification

S. aureus ATCC 43300 was used to prepare 50S ribosomal subunit the same way as described previously.[24,25] Cells were grown in Brain Heart Infusion broth overnight at 37 ℃ and harvested at an OD_{600} of 1.5. Cells were washed twice with 10 mM Tris-HCl pH 7.5, and resuspended in 5 mL buffer A (20 mM HEPES-HCl pH 7.5, 100 mM NH_4Cl, 21 mM Mg $(OAc)_2$, 1 mM EDTA, 1 mM DTT). Cells were broken by an ultrasound crusher. The lysate was centrifuged at 20 000*g* for 90 min to clear cell debris.

The solution layered on a 15 mL of a sucrose cushion (10 mM Hepes-KOH pH 7.5, 500 mM KCl, 25 mM $Mg(OAc)_2$, 1.1 M Sucrose, 0.5 mM EDTA, 1 mM DTT). Centrifugation was subsequently carried out at 45 000 rpm for 15 h using ultracentrifuge Beckman, Type 70Ti rotor. The crude ribosome pellet was resuspended in buffer E (10 mM Hepes-KOH pH 7.5, 100 mM KCl, 10 mM $Mg(OAc)_2$, 0.5 mM EDTA, 1 mM DTT), then layered on 9 mL of 7–30% sucrose gradient and centrifuged in ultracentrifuge Beckman, type SW40Ti rotor,17 100 rpm, 15 h. The gradient was analyzed on the AKTAexplorer system. The fractions corresponding to 50S ribosomal subunit were collected and further subjected to precipitation by PEG20 000. The 50S ribosomal subunit pellet was gently dissolved in 200 μL of storage buffer (10 mM HEPES-HCl pH 7.5, 15 mM KCl, 60 mM NH_4Cl, 10 mM $Mg(OAc)_2$, 1 mM DTT) and stored at −80 ℃.

4.8. SPR interaction and affinity analysis

SPR affinity analysis was performed at 4 ℃ on the bScreen LB 991 Label-free Microarray System (Berthold Technologies, Germany) and Biodot AD-1520 Array Printer (BIODOT Inc., USA) with Photo-cross-linker SensorCHIP™. Concentrations of each compound were diluted to 100 μM with DMSO as the printing working solution for immobilization. A Biodot AD-1520 Array Printer was used to print samples and controls on the photo-cross-linker sensor chip. Each sample was printed four times repeatedly. In order to check the chip quality and whether the detection system works normally, rapamycin was used as a system positive control, and DMSO as a negative control, respectively. Twelve positive control dots were divided into four groups and printed on the four corners of the sensor chip. The sensor chip was dried in vacuum after the array print and quickly transferred to a spectroirradiator for a photocross-linking reaction. Subsequently, the sensor chip was washed with DMF, C_2H_5OH and H_2O for 15 min in turn and evaporated in a N_2 atmosphere. Then, the Flowcell Cover were assembled.

The 50S ribosome was diluted separately with PBST (pH 7.4, 0.1% Tween 20) to 200 nM, 400 nM, 800 nM, 1600 nM and 3200 nM. Different concentration ribosome solutions were injected for 600 s at a flow rate of 0.5 $\mu L \cdot s^{-1}$ at associating stage at 4 ℃, followed by PBST for 360 s at a flow rate of 0.5 $\mu L \cdot s^{-1}$ at each dissociating stage. Then, the surface was regenerated with Glycine-HCl (pH 2.0) for 300 s at a flow rate of 2 $\mu L \cdot s^{-1}$. To validate detection of the compound-protein interactions, we arranged tiamulin as positive control, penicillin and DMSO as negative control and designed kinetic constant tests with FKBP12 after the sample tests.

The raw data of the binding process of compounds and the 50S ribosome were recorded in real time. Compare the response unit (RU) of surface resonance to determine the different binding affinity between each sample dot. The process and analysis of association rate constants (K_a) and dissociation rate constants (K_d) and the equilibrium dissociation constant (K_D, K_d/ K_a) were performed using the data analysis software of

the bScreen LB 991 Label-free Microarray System according to a single-site binding model (1:1 Langmuir binding) with mass transfer limitations for binding kinetics determination.

4.9. Molecular modeling

In order to reveal the binding modes of synthesized pleuromutilin analogues, docking was performed based on the crystal structure of *S. aureus* 50S ribosomal in complex with lefamulin (PDB ID code: 5HL7).[26] The peptidyl transferase center (PTC) model was built that consists of all residues within 40 Å around the lefamulin in 5HL7. The binding site of lefamulin in 5HL7 was set to the docking position. All compounds were prepared with Avogadro 1.1.1.[27] with a 5000 steps Steepest Descent as well as 1000 steps ConJugate Gradients geometry optimization using MMFF94 force field. Docking experiments were performed using the AutoDockTools and Pymol.

Declaration of Competing Interest

The authors declare that they have no known competing financial interests or personal relationships that could have appeared to influence the work reported in this paper.

Acknowledgments

This work was supported by the National Key Research and

Development Program of China (No. 2016YFD0501300), the Guangdong Natural Science Funds for Distinguished Young Scholar (No. 2019B151502002) and the Guangdong Special Support Program innovation team (No. 2019BT02N054).

Appendix A. Supplementary material

Supplementary data to this article can be found online at https://doi.org/10.1016/j.bmc.2021.116138.

References

1 Tenover FC, et al. Characterization of a strain of community- associated methicillin-resistant Staphylococcus aureus widely disseminated in the United States. *J. Clin. Microbiol.* 2006;44:108–118. https://doi.org/10.1128/JCM.44.1.108-118.2006.

2 Klevens RM, Morrison MA, Nadle J, et al. Invasive methicillin-resistant staphylococcus aureus infections in the united states. *JAMA*. 2007;298:1763–1771. https://doi.org/10.1001/jama.298.15.1763.

3 Sader HS, et al. Antimicrobial susceptibility of Gram-positive bacteria isolated from European medical centres: results of the Daptomycin Surveillance Programme (2002–2004). *Clin Microbiol Infect.* 2006;12:844–852. https://doi.org/10.1111/j.1469-0691.2006.01550.x.

4 Sit PS, Teh CSJ, Idris N, Ponnampalavanar S. Methicillin-resistant Staphylococcus aureus (MRSA) bacteremia: Correlations between clinical, phenotypic, genotypic characteristics and mortality in a tertiary teaching hospital in Malaysia. *Infect Genet Evol*. 2018;59:132–141. https://doi.org/10.1016/j.meegid.2018.01.031.

5 Sovari SN, Vojnovic S, Bogojevic SS, et al. Design, synthesis and in vivo evaluation of 3-arylcoumarin derivatives of rhenium(I) tricarbonyl complexes as potent antibacterial agents against methicillin-resistant Staphylococcus aureus (MRSA). *Eur J Med Chem*. 2020;205:112533. https://doi.org/10.1016/j.ejmech.2020.112533.

6 Kavanagh F, Hervey A, Robbins WJ. Antibiotic substances from basidiomy-cetes: VIII. Pleurotus multilus (Fr.) sacc. And Pleurotus passeckerianus pilat. *Proc Natl Acad Sci*. 1951;37:570–574. https://doi.org/10.1073/pnas.37.9.570.

7 Kavanagh F, Hervey A, Robbins WJ. Antibiotic substances from basidiomy-cetes: IX. Drosophila subtarata. (Batsch ex Fr.) quel. *Proc Natl Acad Sci*. 1952;38:555–560. https://doi.org/10.1073/pnas.38.7.555.

8 Hogenauer G. The mode of action of pleuromutilin derivatives location and properties of the pleuromutilin binding site on *Escherichiu coli* ribosomes. *Eur J Biochem*. 1974;52:93–98. https://doi.org/10.1111/j.1432-1033.1975.tb03976.x.

9 Woodford N, Afzal-Shah M, Warner M, Livermore DM. In vitro activity of retapamulin against Staphylococcus aureus isolates resistant to fusidic acid and mupirocin. *J Antimicrob Chemoth*. 2008;62:766–768. https://doi.org/10.1093/jac/dkn266.

10 Goethe O, Heuer A, Ma X, Wang Z, Herzon SB. Antibacterial properties and clinical potential of pleuromutilins. *Nat Prod Rep*. 2019;36:220–247. https://doi.org/10.1039/c8np00042e.

11 Daum RS, Kar S, Kirkpatrick P. Retapamulin. *Nat Rev Drug Disc*. 2007;6:865–866. https://doi.org/10.1038/nrd2442.

12 Lee YR, Jacobs KL. Leave it to lefamulin: a pleuromutilin treatment option in community-acquired bacterial pneumonia. *Drugs*. 2019;79:1867–1876. https://doi.org/10.1007/s40265-019-01219-5.

13 Gao ML, Zeng J, Fang X, et al. Design, synthesis and antibacterial evaluation of novel pleuromutilin derivatives possessing piperazine linker. *Eur J Med Chem*. 2017;127:286–295. https://doi.org/10.1016/j.ejmech.2017.01.004.

14 Jin Z, Wang L, Gao H, Zhou Y, Liu Y, Tang Y. Design, synthesis and biological evaluation of novel pleuromutilin derivatives possessing acetamine phenyl linker. *Eur J Med Chem*. 2019;181:111594. https://doi.org/10.1016/j.ejmech.2019.111594.

15 Zhang Z, Li K, Zhang G, Tang Y, Jin Z. Design, synthesis and biological activities of novel pleuromutilin derivatives with a substituted triazole moiety as potent antibacterial agents. *Eur J Med Chem*. 2020;204:112604. https://doi.org/10.1016/j.ejmech.2020.112604.

16 Gomaa HAM, El-Sherief HAM, Hussein S, et al. Novel 1,2,4-triazole derivatives as apoptotic inducers targeting p53: synthesis and antiproliferative activity. *Bioorg Chem*. 2020;105:104369. https://doi.org/10.1016/j.bioorg.2020.104369.

17 Shang R, Pu X, Xu X, et al. Synthesis and biological activities of novel pleuromutilin derivatives with a substituted thiadiazole moiety as potent drug-resistant bacteria inhibitors. *J Med Chem*. 2014;57:5664–5678. https://doi.org/10.1021/jm500374c.

18 Moreno-Fuquen R, Hincapié-Otero MM, Becerra D, Castillo J, Portilla J, Macías MA. Synthesis of 1-aroyl-3-methylsulfanyl-5-amino-1,2,4-triazoles and their analysis by spectroscopy X-ray crystallography and theoretical calculations. *J Mol Struct*. 2021;1226:129317. https://doi.org/10.1016/j.molstruc.2020.129317.

19 Ahmad I, Huang L, Hao H, Sanders P, Yuan Z. Application of PK/PD modeling in veterinary field: dose optimization and drug resistance prediction. *Biomed Res Int*. 2016;2016:5465678. https://doi.org/10.1155/2016/5465678.

20 Wang JJ, Guo JJ, Zhan J, Bu HZ, Lin JH. An in-vitro cocktail assay for assessing compound-mediated inhibition of six major cytochrome P450 enzymes. *J Pharm Anal*. 2014;4:270–278. https://doi.org/10.1016/j.jpha.2014.01.001.

21 Zhang G, Zhang Z, Li K, et al. Design, synthesis and biological evaluation of novel pleuromutilin derivatives containing piperazine and 1,2,3-triazole linker. *Bioorg Chem*. 2020;105, 104398. https://doi.org/10.1016/j.bioorg.2020.104398.

22 Stresser DM, Broudy MI, Ho T et al. Highly selective inhibition of human cyp3a in vitro by azamulin and evidence that inhibition is irreversible, Drug Metabol Dispos 32 (2004) 105e112, https://doi.org/10.1124/dmd.32.1.105.

23 Xu C, Qi Y, Cui Z et al. Discovery of novel elongator protein 2 inhibitors by compound library screening using surface plasmon resonance. RSC Adv 2019;9:1696-1704, http://xlink.rsc.org/?DOI=C8RA09640F.

24 Iskander K, Quentin V, Anthony B, et al. Structure of the 70S ribosome from human pathogen Staphylococcus aureus[J]. Nucl Acids Res 2017(2):1026–1026, https://doi.org/10.1093/nar/gkw1126.

25 Lolk L, PHlsgaard J, Jepsen AS, et al. A click chemistry approach to pleuromutilin conjugates with nucleosides or acyclic nucleoside derivatives and their binding to the bacterial ribosome [J]. J Med Chem 51(16);2008:4957–67, https://doi.org/10.1021/jm800261u.

26 Eyal Z, Matzov D, Krupkin M, et al. A novel pleuromutilin antibacterial compound, its binding mode and selectivity mechanism. *Sci Rep*. 2016;6:39004. https://doi.org/10.1038/srep39004.

27 Hanwell MD, Curtis DE, Lonie DC, et al. Avogadro: an advanced semantic chemical editor, visualization, and analysis platform. *J Cheminform*. 2012;4:17. https://doi.org/10.1186/1758-2946-4-17.